Supplementary Information

Chemical and structural insights of the nano organo-mineral interfaces in growing abalone nacre

Widad Ajili,[1,2] Marta de Frutos,[3] Imène Estève,[4] Marie Albéric,[1] Nicolas Menguy,[4] Karim Benzerara,[4] Antonio Checa,[5] Stéphanie Auzoux-Bordenave,[2]* Thierry Azaïs,[1]* and Nadine Nassif,[1]*

[1] *Sorbonne Université, CNRS, Collège de France, Laboratoire de Chimie de la Matière Condensée de Paris (LCMCP), 4, place Jussieu, F-75005, Paris, France.*

[2] *Laboratoire de Biologie des Organismes et Ecosystèmes Aquatiques" (BOREA), Muséum national d'histoire naturelle/CNRS/IRD/Sorbonne Université/UCN/UA/Station Marine de Concarneau, 29900 Concarneau, France*

[3] *Laboratoire de Physique des Solides, Université Paris-Saclay, CNRS UMR 8502, F-91405 Orsay.*

[4] *Sorbonne Université, Muséum National d'Histoire Naturelle, UMR CNRS 7590, IRD, Institut de Minéralogie, de Physique des Matériaux et de Cosmochimie, IMPMC, 75005 Paris, France*

[5] *University of Granada, Department of Stratigraphy and Paleontology, 18071 Granada, Spain*

* *Corresponding authors: stephanie.auzoux-bordenave@mnhn.fr, thierry.azais@sorbonne-universite.fr, nadine.nassif@sorbonne-universite.fr*

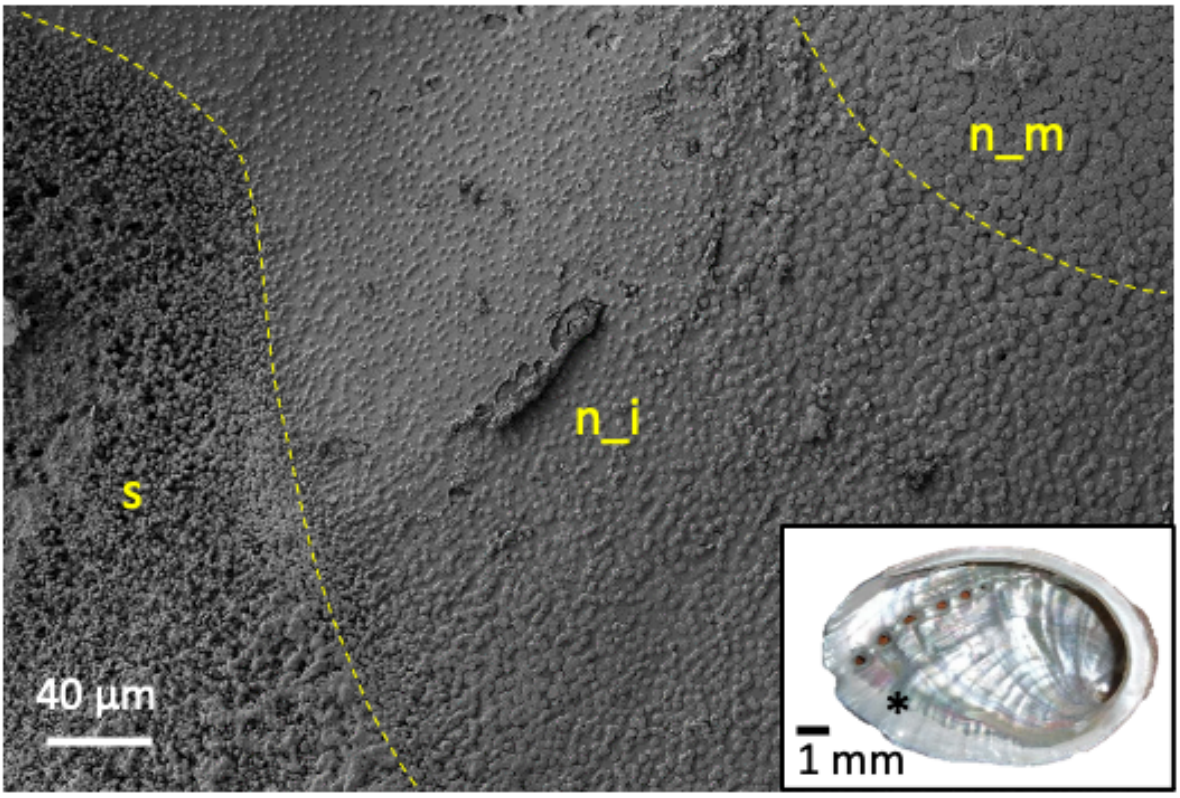

Figure S1. SEM FEG observations of a growing region showing the transition between the spherulitic (s), immature nacre (n_i) and mature nacre (n_m) regions. Inset: one-year-old *Haliotis tuberculata* shell showing the iridescent nacre. The star (*) indicates the growing edge region with the transition between the spherulitic layer and nacre.

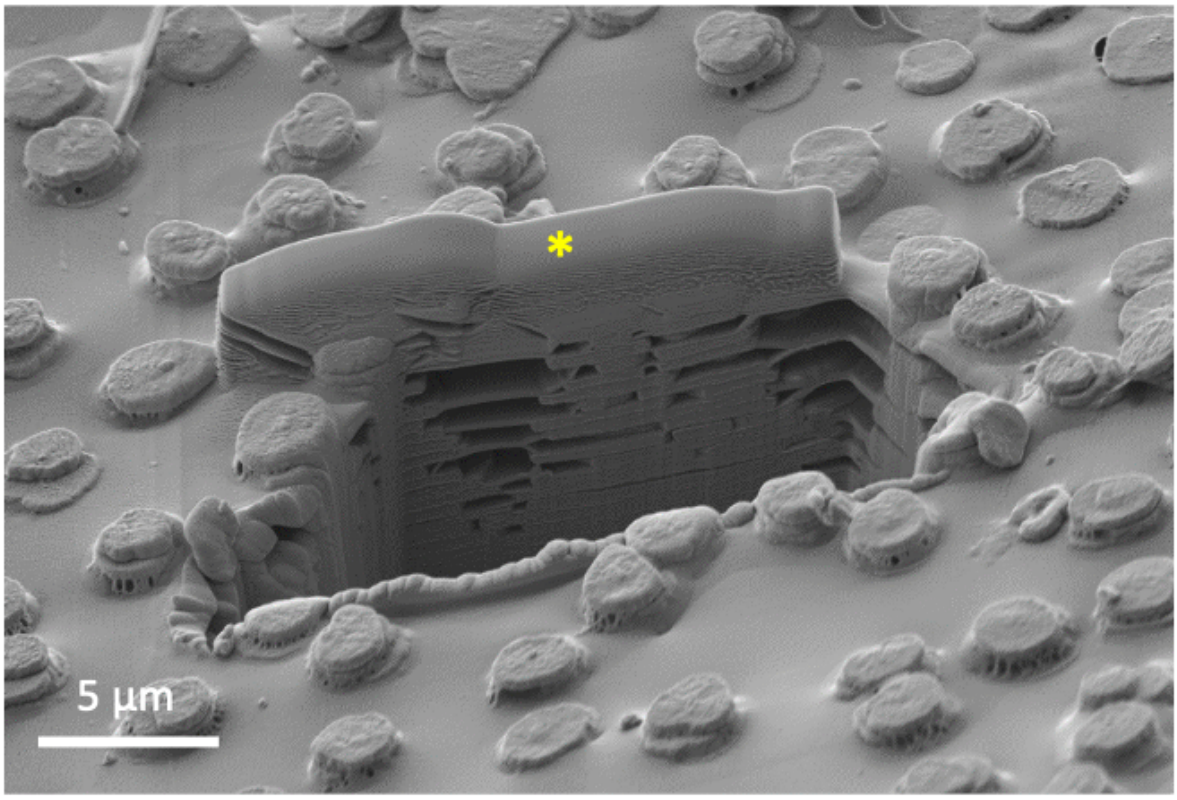

Figure S2. FEG-SEM observations of growing aragonite tablets (immature nacre (n_i)) in *Haliotis tuberculata* after FIB milling. The Pt coating is indicated by a yellow star.

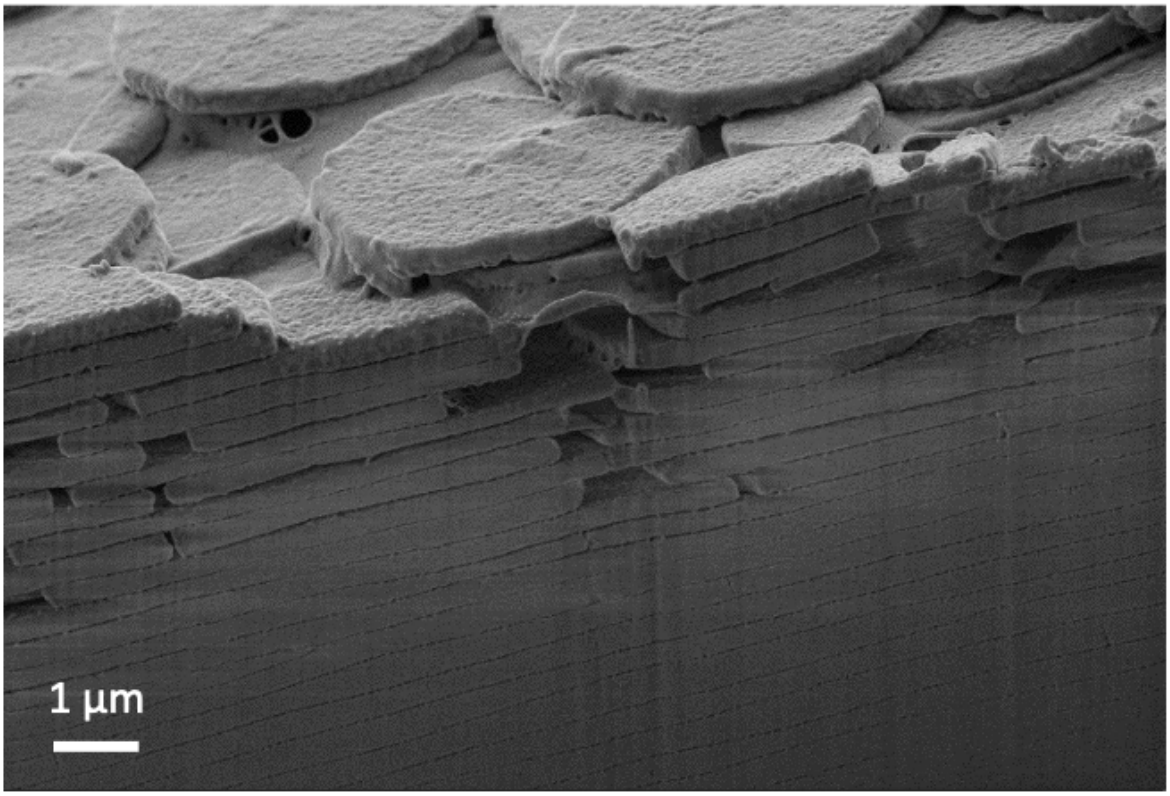

Figure S3. FEG-SEM micrograph of growing aragonite tablets showing FIB milled side-view of mature nacre (n-m).

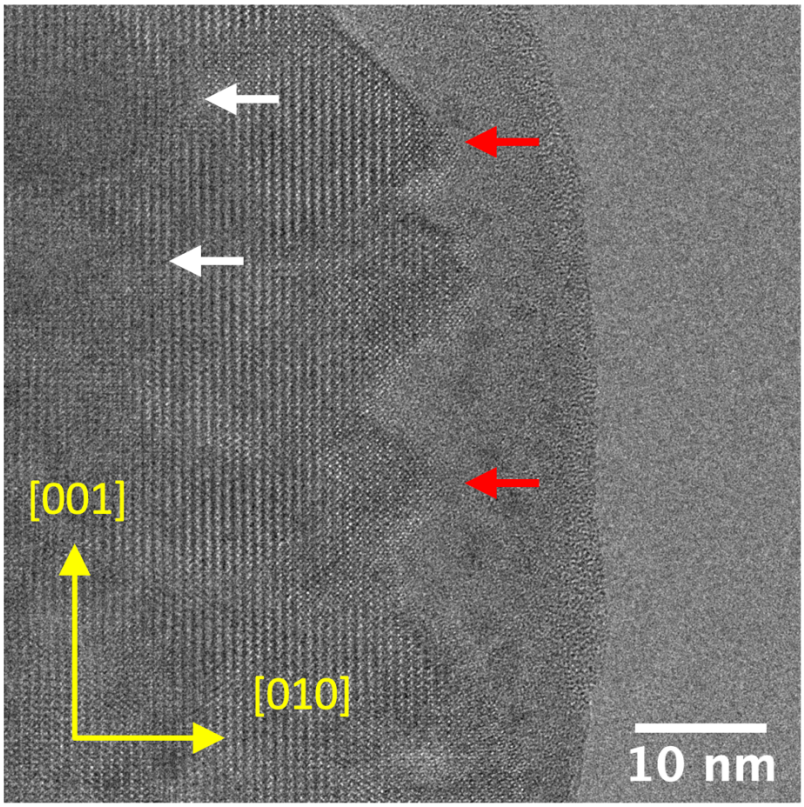

Figure S4. HR-TEM observation of pyramidal nano-growths seen along the vertical face of the platelet. They are found on the surface (red arrows) and inside the crystalline core (white arrows).

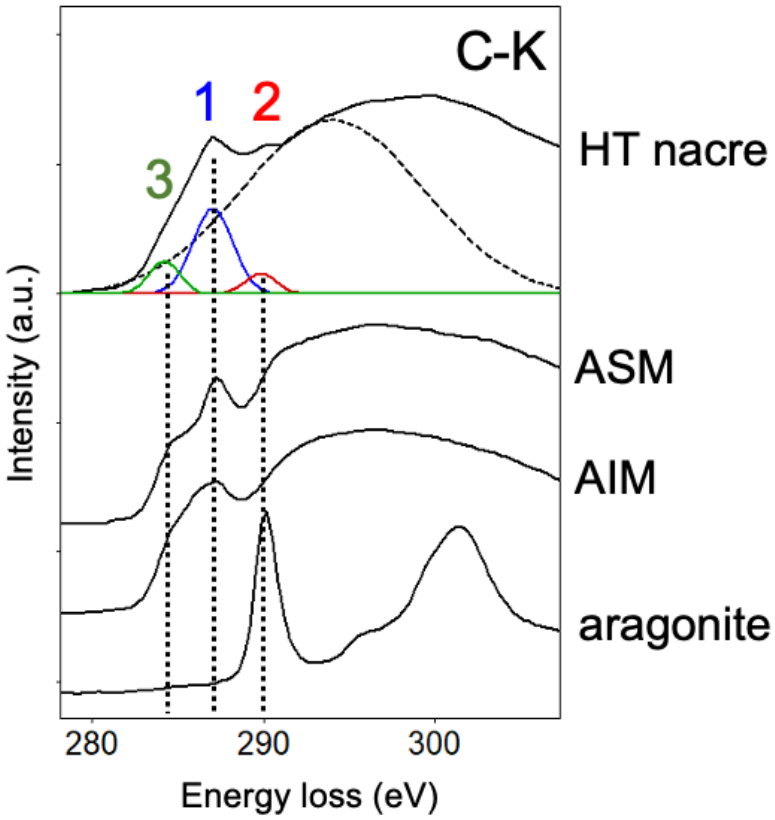

Figure S5. EELS carbon K- edge acquired on different samples. From top to bottom: *Haliotis tuberculata* (HT) nacre, ASM from HT nacre, AIM from HT nacre and synthetic aragonite. The spatial distributions of organic species (proteins and chitin) and carbonate are obtained by fitting the peaks at 287 eV and 290 eV on C-K edge by a Gaussian (respectively blue and red curves labelled 1 and 2).

Text S5. In order to assign the different carbon peaks (detailed in section 3.2 of main text), reference spectra from specific samples were acquired (**Figure S5**): Acidic soluble organic matrix (ASM *i.e.*, purified proteins extracted from HT nacre) and acidic insoluble organic matrix (AIM *i.e.*, resin section of organic matrix from HT nacre) exhibit the narrow peak around 287-288 eV (peak "1" in **Figure S5**). Concerning synthetic aragonite, the carbonate group is characterized by a peak at 290 eV (peak "2" in **Figure S5**) (Brandes *et al*, 2010; doi:10.1107/S0909049510020029). A third peak is also observed at 285 eV (peak "3" in **Figure S5**) as a small shoulder for the ASM and AIM samples. This peak is often assigned to amorphous carbon when samples are deposited on TEM carbon grid but it is also observed for HT nacre FIB thin section. This observation might be due to a partial degradation of the organic compounds under the electron beam leading to amorphous carbon. As a consequence, we assume here that the peaks at 285 and 288 eV are associated with organic species (such as proteins particular). In X-ray absorption measurements, the position of the peak associated to the C 1s $\rightarrow \pi^*$ transition is supposed to be specific to each biomolecule (proteins, lipids, DNA, saccharides) (Lawrence, J. R. et al. *Appl. Environ. Microbiol.* **2003**, *69*, 5543–5554, doi: 10.1128/AEM.69.9.5543-5554.2003). However, compared to XANES, EEL spectra exhibit modified signatures for organic compounds due to beam damage effect. As such we believe that proteins are not distinguishable from chitin in our conditions.

In order to map the organic species and carbonate, a multi-Gaussian fitting was applied to the carbon peaks using the NLLS (non-linear least squares) method in Gatan's Digital Micrograph software. A typical example of multi-Gaussian fit is presented in **Figure S5** for the HT nacre**.** The fitting is repeated for each pixel across the scanned area in a spectrum image. The abundancy of each species is then given by the amplitude of the Gaussian used to fit each peak across the imaged area.

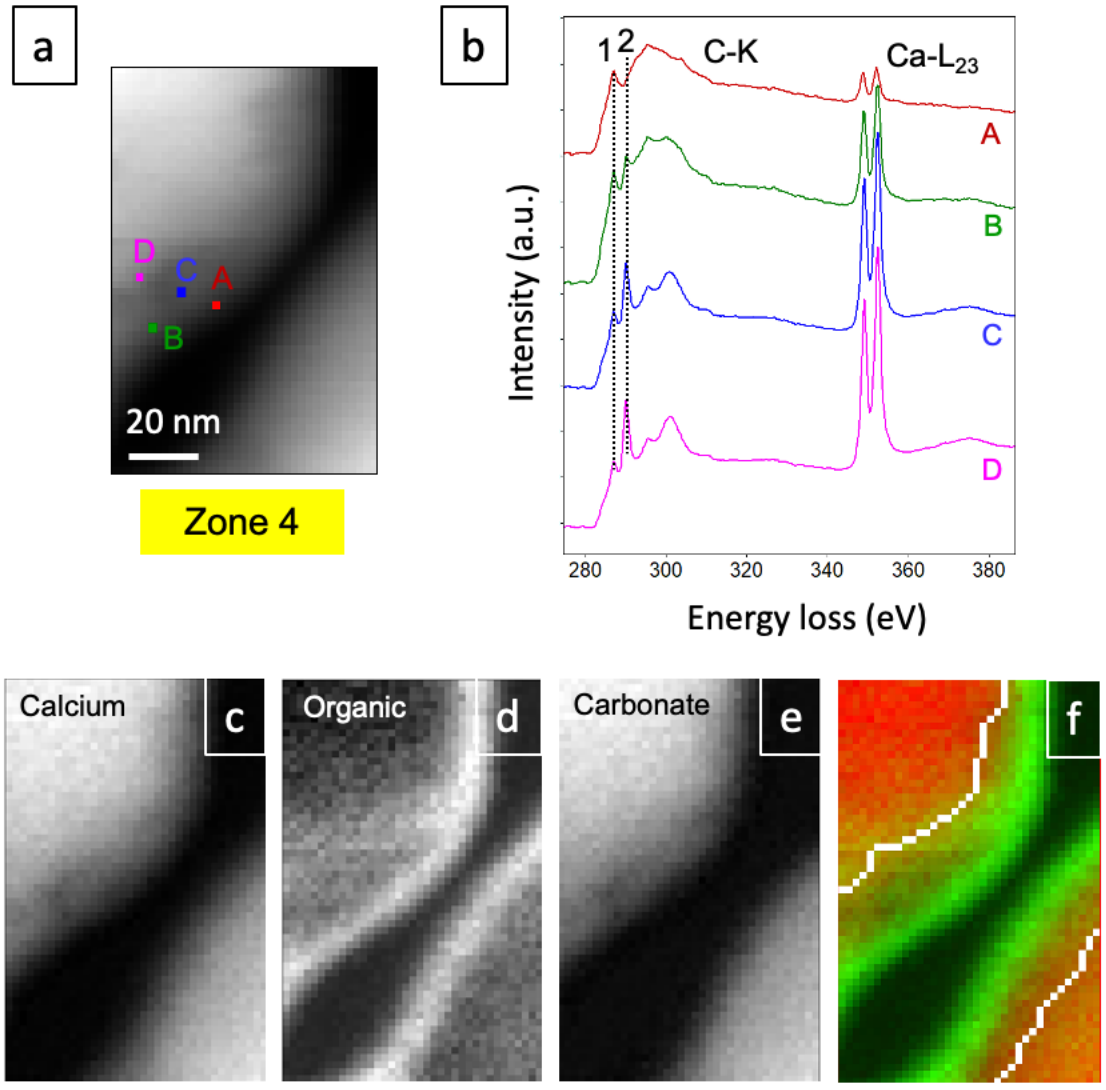

Figure S6. EELS analysis of zone 4 from Figure 5a. a) STEM-HAADF image of the analysed zone, b) EEL spectra at the C-K edge and the Ca-L_{23} edge from positions A, B, C and D in a). The characteristic peaks corresponding to organic (peak 1) and carbonate (peak 2) are marked with dashed lines. (c) EELS map of the distribution of (c) calcium, (d) organic and (e) carbonate deduced from their respective edge signals. (f) Colored image obtained from the individual maps (d) and (e) showing the relative abundancies of organic species (green) compared to carbonate (red). The white line in (f) corresponds to the detection limit of EELS signal due to sample thickness.

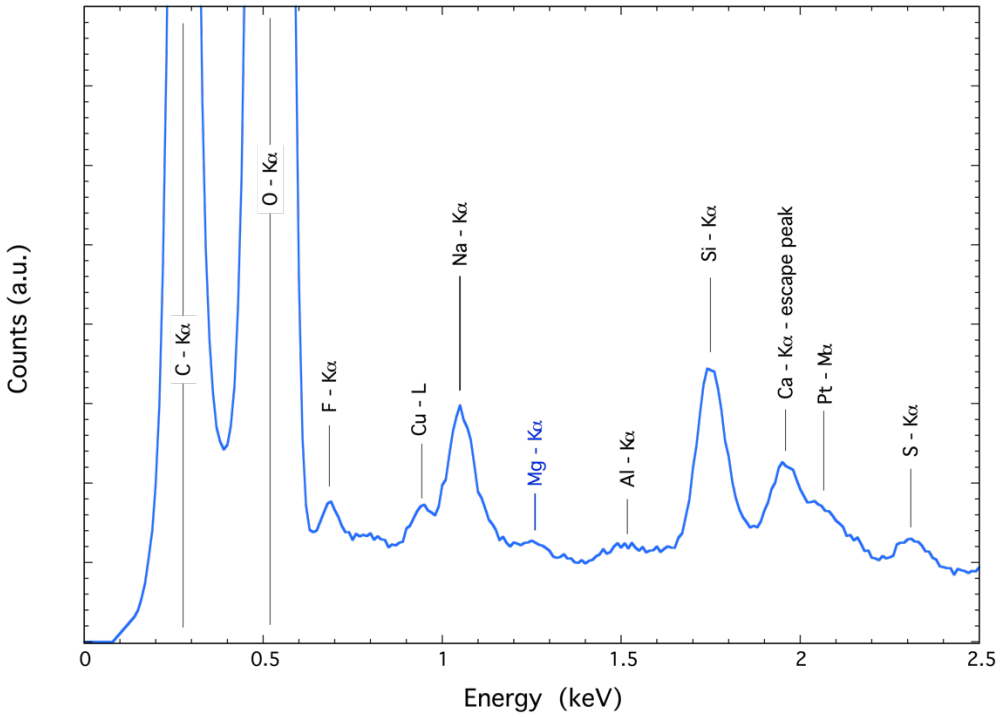

Figure S7. EDX analysis performed on the lateral surface layer of growing aragonite tablets showing that Mg is not detected.

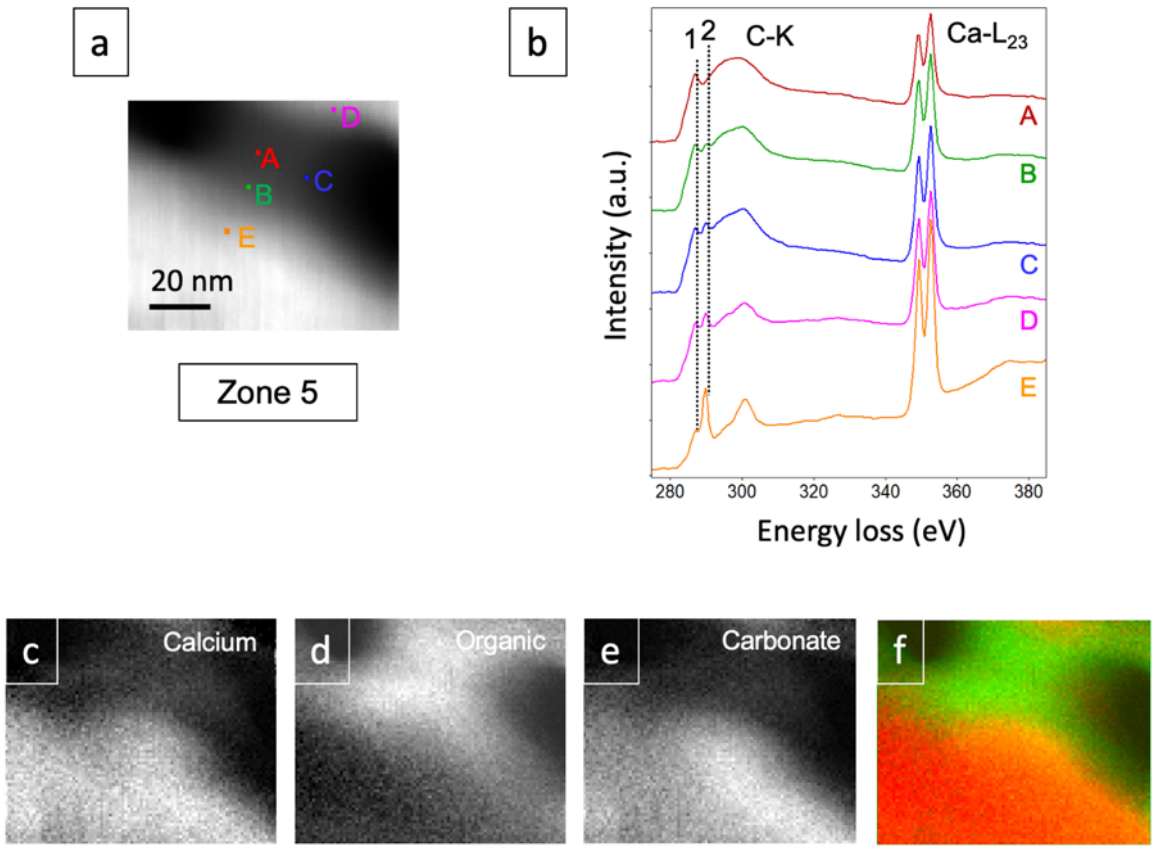

Figure S8. EELS analysis of zone 5 from Figure 5a. a) STEM-HAADF image of the analysed zone, b) EEL spectra at the C-K edge and the Ca-L_{23} edge from positions A, B, C, D and E in a). The characteristic peaks corresponding to organic (peak 1) and carbonate (peak 2) are marked with dashed lines. (c) EELS map of the distribution of (c) calcium, (d) organic and (e) carbonate deduced from their respective edge signals. (f) Colored image obtained from the individual maps (d) and (e) showing the relative abundancies of organic species (green) compared to carbonate (red).